ISBN: 978-3-95450-184-7 doi:10.18429/JACoW-IPAC2018-THXGBE1

6D BEAM MEASUREMENT, CHALLENGES AND POSSIBILITIES*

A.V. Aleksandrov, S. Cousineau, A. Zhukov, ORNL, Oak Ridge, TN 37830, USA
B. Cathey, University of Tennessee, Knoxville, TN 37966, USA

Abstract

A system to measure the full 6D beam parameters was built at the SNS Beam Test Facility (BTF). Such a measurement will allow detailed analysis of the beam physics from a properly measured input term. This invited talk provides an overview of the principles and design of this system, and reports on its status and results.

INTRODUCTION

Particle tracking simulation is an important tool for the study of beam dynamics in hadron linacs. It is highly desirable for simulation tools to accurately predict not only RMS properties but also details of the beam distribution. Because linacs are not a closed loop, the beam dynamics are intimately dependent on the initial beam entering the system. Logically, without knowing this distribution, there should be no expectation that simulations will accurately predict the beam evolution.

A particle at the linac entrance is described by six independent degrees of freedom. In a Cartesian coordinate system, they are: the horizontal and vertical positions and their conjugate momentum x, p_x, y, p_y, and the energy and phase relative to a design reference particle w, φ. Thus, a beam is fully described by its distribution of particles in the 6D phase space, and a complete measurement of a distribution must include all six dimensions and their cross-correlations.

Traditional beam diagnostics only measure projections of the phase space in one, two, or at most four dimensions. Typically, the two-dimensional projections $f_x(x, x')$, $f_y(y, y')$, and $f_z(w, \varphi)$ of the six-dimensional distribution $f_6(x, x', y, y', w, \varphi)$, called "emittances", are measured independently. To create an initial distribution for simulations, these 2D projections are assembled together with the assumption that there are no correlations between the degrees of freedom:

$$f_6 = f_x \cdot f_y \cdot f_z \qquad (1)$$

This equation is the definition of *uncorrelated* distributions and is only true if the degrees of freedom are not dependent. Although the validity of the assumption (1) is often assumed, it is mostly due to a lack of experimental evidence pro or contra. There are many physical mechanisms capable of coupling the degrees of freedom during the beam transport, e.g. fringe fields of the magnetic elements, space charge forces.

The main goal of the project described in this paper was to develop a method for measuring the 6D beam distribution function at the linac entrance. The measured distribution can be used to generate initial coordinates for PIC simulation particles and to check the validity of assumption (1).

A straightforward method for measuring the 6D phase space distribution of a beam was proposed in [1]. Figure 1 illustrates the principle of the method. A set of six movable slits is used to localize particles inside a small area of the 6D phase space: the first pair of orthogonal slits transmits only particles with coordinates within intervals $x \pm \Delta x$, $y \pm \Delta y$; the second pair of orthogonal slits at a set distance from the first pair transmits only particles with angles within intervals $x' \pm \Delta x'$, $y' \pm \Delta y'$; the fifth slit, placed at a location with large energy dispersion created by a bending magnet, transmits only particles with energy within interval $w \pm \Delta w$. The remaining particles pass through an RF deflector, which deflects particles in accordance with their time of arrival. Only particles with arrival phases within the interval $\varphi \pm \Delta\varphi$ are transmitted through the sixth slit. At the end, particles within the interval $\pm\Delta x\Delta x'\Delta y\Delta y'\Delta w\Delta\varphi$ around the point x, x', y, y', w, φ in the 6D phase space are collected by a Faraday cup and their total charge is measured. The distribution function is measured by moving all the slits sequentially to span the whole phase space occupied by the beam. As the scan is sequential it requires n^6 steps, where n is the number of points per each dimension. In practice, a multi-hour scan is required to achieve a reasonable resolution of 10-20 points per dimension. Therefore, the technique is ideally suited for a dedicated facility with significant beam time available for measurement.

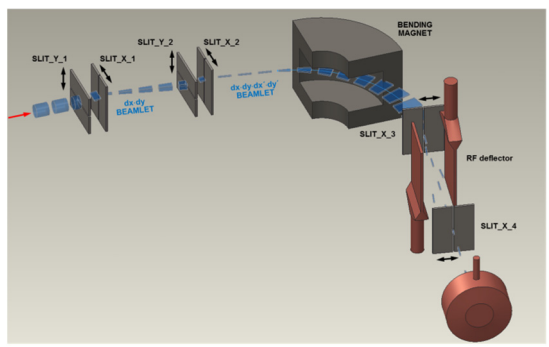

Figure 1: A diagram showing the principle of 6-dimensional phase scan.

* This manuscript has been authored by UT-Battelle, LLC, under Contract No. DE-AC05-00OR22725 with the U.S. Department of Energy. The United States Government retains, and the publisher, by accepting the article for publication, acknowledges that the United States Government retains a non-exclusive, paid-up, irrevocable, world-wide license to publish or reproduce the published form of this manuscript, or allow others to do so, for United States Government purposes. The Department of Energy will provide public access to these results of federally sponsored research in accordance with the DOE Public Access Plan (http://energy.gov/downloads/doe-public-access-plan).

ISBN: 978-3-95450-184-7 doi:10.18429/JACoW-IPAC2018-THXGBE1

REALISATION OF SIX-DIMENSIONAL BEAM PHASE SPACE SCAN

The technique described above was implemented at the SNS Beam Test Facility (BTF), which is a functional duplicate of the Spallation Neutron Source linac Front End [2]. The BTF is capable of producing a pulsed 2.5 MeV H^- ion beam with a peak current of up to 50 mA, pulse width of 50 μs, and repetition rate of 10 Hz when using the beam line diagnostics. The 6D scan hardware design closely followed the Fig. 1 concept with the addition of quadrupole magnets to contain the beam inside the aperture. The layout of the beam line is shown in Fig. 2.

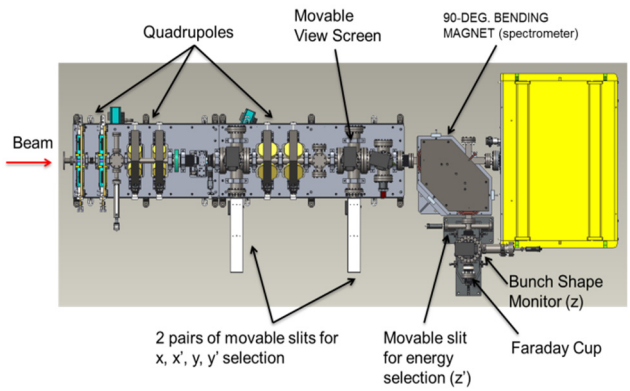

Figure 2: Layout of the SNS BTF beam line with equipment for 6D phase space measurement.

Two pairs of identical 200 μm wide carbon silts, shown in Fig. 3, are used for the transverse scan. The horizontal and vertical slits in each pair are offset by 10 mm longitudinally to allow for independent simultaneous motion without collision.

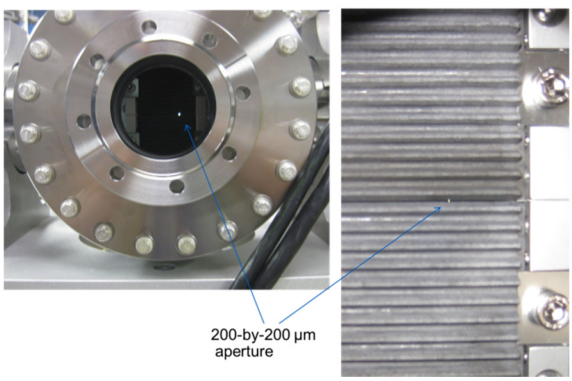

Figure 3: The horizontal and vertical slits pair for transverse phase space scan.

The energy selection slit is made of an alumina ceramic based luminescent material as shown in Fig. 4. This allows measuring the entire energy distribution in one shot by acquiring the screen image with a video camera or selecting a portion of the energy spectrum for temporal analysis farther downstream.

Deflecting the 2.5 MeV H^- ions would require inconveniently large RF power, and therefore the temporal degree of freedom is instead measured by a so-called Beam Shape Monitor (BSM). The BSM time of arrival of secondary electrons produced when the ions strike a tungsten wire in the beam path [3]. Also, in order to reduce the scan time, the time resolving slit is replaced with a luminescent screen and video camera so that the whole temporal profile is measured in one pulse. The modified BSM hardware is shown in Fig. 5.

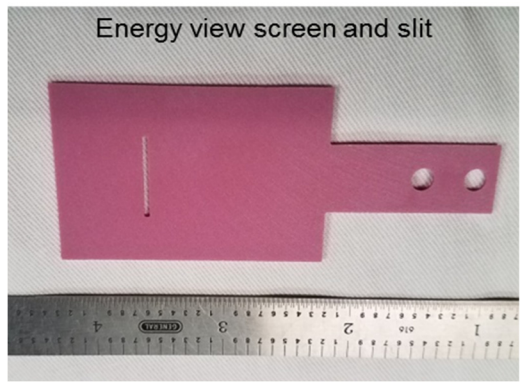

Figure 4: The energy selection slit.

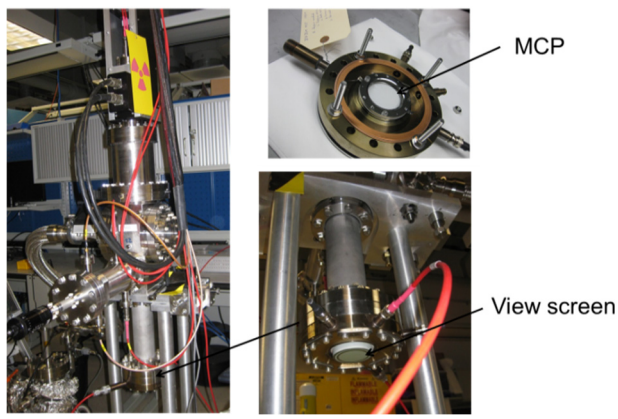

Figure 5: The modified Beam Shape Monitor hardware.

The RMS beam envelopes from the RFQ exit to the BSM wire are shown in Fig. 6. The bunch is well contained horizontally but freely expands longitudinally due to an absence of longitudinal focusing in the beam line. The longitudinal RMS size of about 20 mm becomes comparable to the bunch-to-bunch distance of 54 mm at the BSM location causing the bunches to overlap in the time domain as illustrated in Fig. 7. The overlapping would create a problem for a 1D measurement to resolve the temporal structure. However, bunches do not overlap in the 2D domain $w - \varphi$ as illustrated in Fig. 8. The seemingly overlapping parts of the bunches have different energies and therefore can be separated using the energy selection slit. An example of measured longitudinal profiles for different energy slices is shown in Fig. 9. The longitudinal emittance is constructed by combining the measurements for all energy slit positions as shown in Fig. 10.

ISBN: 978-3-95450-184-7 doi:10.18429/JACoW-IPAC2018-THXGBE1

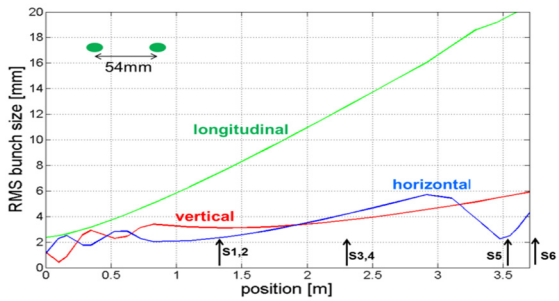

Figure 6: The RMS beam envelopes' evolutions from the RFQ exit to the end of the beam line.

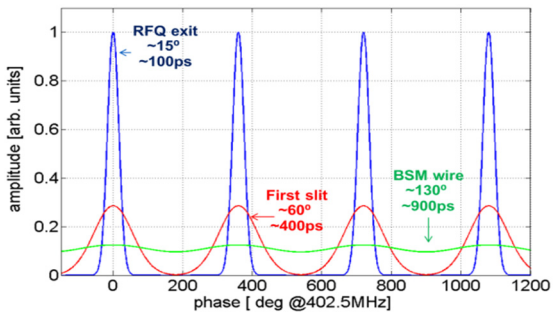

Figure 7: Evolution of the longitudinal bunch shape from the RFQ exit to the end of beam line.

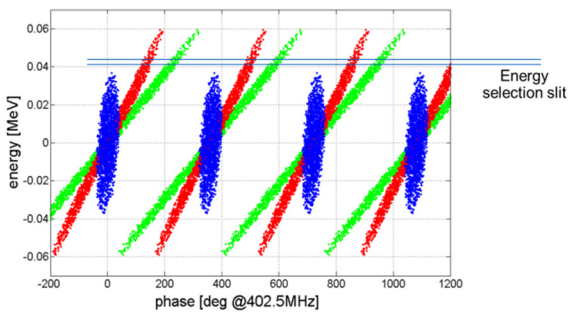

Figure 8: Evolution of the particle distribution on the energy-time plain from the RFQ exit (blue) to the first slit location (red) and end of the beam line (green).

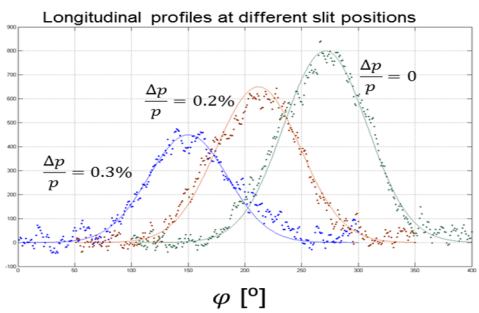

Figure 9: Measured longitudinal bunch profiles for different energy slit locations.

The total 6D phase space is scanned by moving 5 slits sequentially and saving the longitudinal profiles for each slit position. The beam parameters remain stable during the scan as illustrated in Fig. 11 where plot of the beam current at the RFQ exit is shown during 32 hours of the scan. Measurements for several abnormal pulses observed on the plot are excluded from the final data analyses. The beam current stability is a good indicator of stability for all beam parameters based on many years of experience with the SNS Front End.

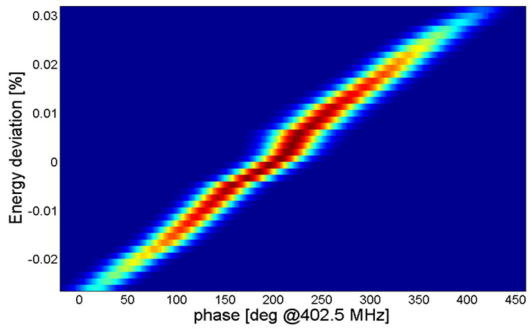

Figure 10: The longitudinal emittance combined from many longitudinal profiles measured at different energy slit positions.

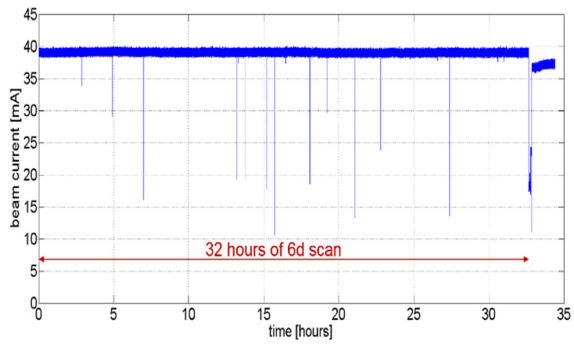

Figure 11: Beam current at the RFQ exit during the 6D scan.

DATA ANALYSIS

The measured 6D data can be used to generate an input set of particle initial coordinates for computer simulations, but higher resolution is desirable for an accurate simulation. More importantly, the experimental data allow an opportunity to explore the internal structure of the full phase space distribution, and specifically to check for correlations between coordinates in all six degrees of freedom. There is no proven technique for finding arbitrary correlations in high-dimensional spaces. The linear correlation coefficients can be calculated for all combinations of the six degrees of freedom, but even zero values for the correlation coefficients do not guarantee the absence of higher order correlations, and a correlation of any order invalidates equation (1). Full exploration of this problem remains to be done.

As a first step, a visual inspection of various 1D and 2D projections and "partial projections" of the 6D distribution was conducted. The following definitions are used in the data analysis discussion below.

Full projections are reduced dimensionality distribution functions obtained by integrating over all unused coordinates. For example, a partial projection on a 2D plane is:

ISBN: 978-3-95450-184-7 doi:10.18429/JACoW-IPAC2018-THXGBE1

$$f(a,b) = \int_{-\infty}^{\infty} f_6(a,b,\bar{x})d\bar{x}. \quad (2)$$

On the other hand, partial projections are reduced dimensionality distribution functions obtained by fixing some coordinates to constant values and integrating over others. For example, a projection on 2D plane is:

$$p(a,b) = \int_{-\infty}^{\infty} f_6(a,b,\overline{v} = \overline{v_0},\bar{x})d\bar{x}. \quad (3)$$

In the formulas above a, b are any coordinates from the x, x', y, y', w, φ set; $\overline{v}$ is a vector of coordinates remaining in the x, x', y, y', w, φ set after a, b are removed; $\overline{x}$ is the vector of coordinates remaining in the x, x', y, y', w, φ set after a, b and $\overline{v}$ are removed. Vector $\overline{v}$ is equal to the vector $\bar{v}_0$, which is the fixed coordinates for the partial projection. A partial projection can be measured directly by leaving the slits responsible for fixed coordinates at fixed positions. These scans are much faster than full 6D scans and allow exploring identified correlations in reasonable time.

EXPERIMENTAL RESULTS

A clearly visible correlation was found between the transverse degrees of freedom and the energy. Fig. 12 shows a 2D color map of the $f(x', w)$ partial projection with $x = y = y' = 0$ and integrated over φ. A dependence of the w distribution upon the angle value x' is obvious in the plot. The w distribution showed similar dependence with x, y, and y' as well.

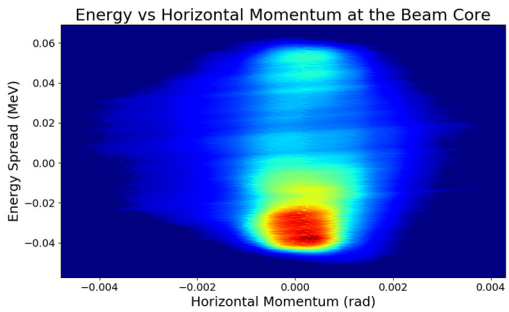

Figure 12: Partial projection of the 6D distribution on the energy-horizontal angle plane.

The plots in Fig. 13 show 1D partial projections with different numbers of fixed coordinates: the green line shows the energy spectrum measured with $x = x' = 0$ and integrated over y, y', φ; the red line shows the energy spectrum measured with $x = x' = y = 0$, integrated over y', φ; and the blue line shows the energy spectrum measured with $x = x' = y = y' = 0$, integrated over φ. The plots demonstrate the necessity of performing scans in at least 4D for the correlation to become visible, and in 5D for resolving the details.

The plots in Fig. 14 show 1D partial projections with four fixed coordinates $x = x' = y = y' = 0$ measured for beam currents of 40 mA, 30 mA, and 20 mA. The correlation is well pronounced at 40 mA, becomes less visible with a smaller beam current of 30 mA, and completely disappears at 20 mA. The beam current dependence demonstrates that the observed correlation is created by the Coulomb forces within the distribution.

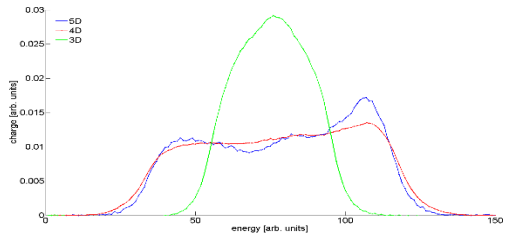

Figure 13: Plots of 1D partial projections on the energy axis with different number of variables integrated. The plots are the results of integration over three (green), two (red) and one (blue) degrees of freedom.

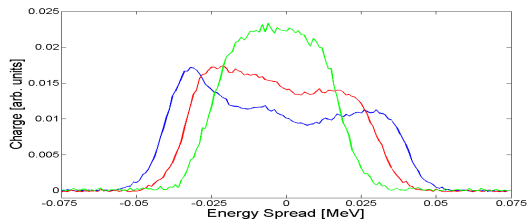

Figure 14: Plots of 1D partial projections on the energy axis measured at different beam currents, 40 mA (blue), 30 mA (red), and 20 mA (green).

COMPUTER SIMULATION

A simple computer simulation was used to confirm the space charge forces ability to create correlations in the distribution function like the one observed in the 6D measurements. A 1m long transport line consisting of drifts and four quadrupole magnets arranged similarly to the first 1 m of the BTF beam line was simulated using PARMILA PIC code. An ideal 6D Gaussian function was used to generate the initial particle coordinates. A partial projection on the $w - x$ plane of the distribution function at the beam line exit is shown in Fig. 15. A pattern similar to the one in the Fig. 12 is clearly visible.

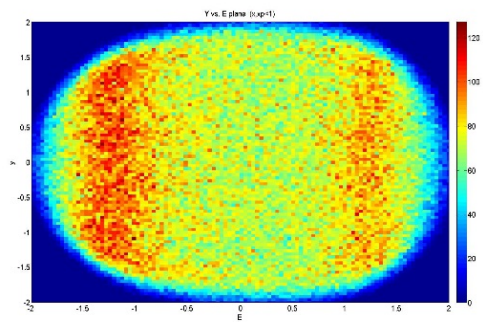

Figure 15: Partial projection of the simulated 6D distribution on the energy-vertical position plane.

ISBN: 978-3-95450-184-7 doi:10.18429/JACoW-IPAC2018-THXGBE1

1D partial projections simulated with different beam currents are shown in Fig. 16. The simulation results confirm that space charge forces are responsible for the observed correlations in the distribution function.

CONCLUSIONS AND FUTURE PLANS

The first full 6D phase space measurement of an accelerator beam has been completed. The high dimensionality scans showed a previously unknown correlation between degrees of freedom. These results indicate equation (1) is an invalid representation of the beam phase space distribution and high dimensionality measurements are required to accurately represent the distribution. To study the impact of the observed correlation on the beam evolution experimentally the following R&D activities are planned: reduce the 6D scan time to allow for higher resolution and/or multiple scans at different beam parameters, develop methods for multi-dimensional data analysis, and build a test beam line to allow the benchmarking of different methods of generating input distributions for computer simulations against the direct measurement.

Decreasing the Scan Time

The maximum beam pulse repetition rate of ~2.5 Hz achieved during the 6D scan was limited by the slit motion velocity and the image data acquisition time. It is straightforward to optimize the both for full utilization of the maximum BTF pulse rate of 10 Hz, which should reduce the total scan time by about a factor of 4.

About 80% of points in the measured 6D scan data have zero value. This means the scanned 6D volume is larger than volume occupied by the beam. The scanning algorithm can be optimized to better "envelope" the beam volume. An estimate of potential saving in number of sampled points is the ratio of 6D cube to 6D sphere volumes

$$\frac{V_{\square}}{V_{\circ}} = \frac{\Gamma(4)\cdot 64}{\pi^3} \approx 12.$$

The full optimization is probably not achievable but a factor of 2-3 in scan time reduction should be possible with proper optimization.

Further improvement can be achieved by eliminating the energy selection slit and placing the BSM wire at its location. In this case the 2D energy-phase image can be acquired in one pulse, providing another order of magnitude reduction of the scan time. This change requires significant redesign of the BSM hardware and modification of the beam line optics.

The FODO Beam Dynamics Experiment

An extension of the BTF beam line will be added, as shown in Fig. 16, to provide a test bench for experimental verification of beam dynamics simulation codes.

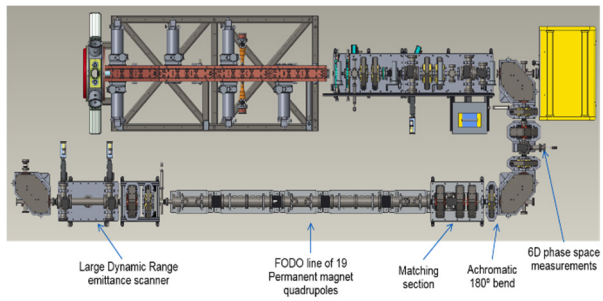

Figure 16: A layout of the FODO beam line for high intensity beam dynamics studies at the SNS BTF.

The extension consists of 19 quadrupole magnets in a FODO arrangement. The magnets are made of permanent magnetic material and reside within a vacuum pipe as shown in Fig. 17. A matching section of five quadrupole electromagnets allows to control the beam matching conditions at the FODO line entrance. A slit-slit 4D emittance measurement station at the FODO line exit allows for phase space distribution measurements with a high dynamic range of $10^5 - 10^6$. Together with the 6D phase space scanner at the RFQ exit, the new beam line provides a complete tool for codes benchmarking: initial distribution measurement, transport in a well-defined optical structure, and measurement of the final distribution.

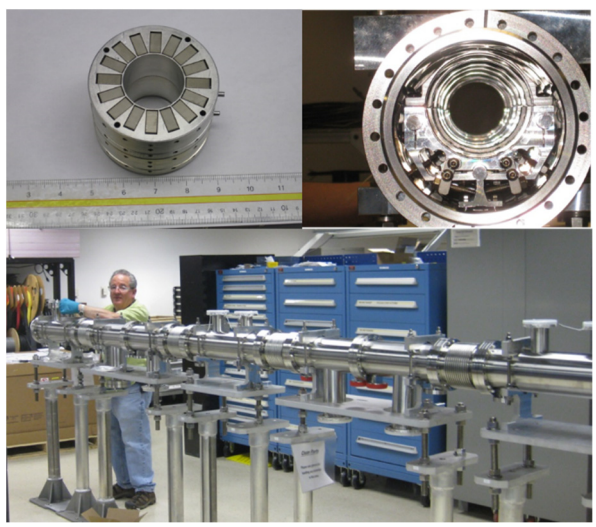

Figure 17: The design of the SNS BTF FODO beam line. The quadrupole permanent magnet is on top left, the magnet mounting structure is on top right, the assembled FODO line is at the bottom of the figure.

ACKNOWLEDGMENTS

This work has been partially supported by NSF Accelerator Science grant 1535312. ORNL is managed by UT-Battelle, LLC, under contract DE-AC05-00OR22725 for the U.S. Department of Energy.

ISBN: 978-3-95450-184-7 doi:10.18429/JACoW-IPAC2018-THXGBE1

REFERENCES

[1] V. Danilov, A. Aleksandrov, "Beam Invariants for Diagnostics", in *Proc. 9th European Particle Accelerator Conf. (EPAC'04)*, Lucerne, Switzerland, Jul. 2004, pp. 1518-1520.

[2] A. Aleksandrov, B. Cathey, S. Cousineau, M. Crofford, B. Han, Y. Kang, A. Menshov, C. Peters, A. Webster, R. Welton, A. Zhukov, "Commissioning of the New SNS RFQ and 2.5 MeV Beam Test Facility", in *Proc. 8th Int. Particle Accelerator Conf. (IPAC'17)*, Copenhagen, Denmark, May 2017, pp. 2438-2440.

[3] A.V. Feschenko, "Methods and Instrumentation for Bunch Shape Measurements", in *Proc. Particle Accelerator Conf. (PAC'01*), Chicago, IL, USA, Jun. 2001, pp. 517-519.